Polyaniline nanofibre supported platinum nanoelectrocatalysts for direct methanol fuel cells

View the article online for updates and enhancements.

Polyaniline nanofibre supported platinum nanoelectrocatalysts for direct methanol fuel cells

Zhongwei Chen, Lianbin Xu, Wenzhen Li, Mahesh Waje and Yushan Yan[1]

Department of Chemical and Environmental Engineering, and College of Engineering—Center for Environmental Research and Technology (CE-CERT), University of California-Riverside, Riverside, CA 92521, USA

E-mail: Yushan.Yan@ucr.edu

Abstract
A novel polyaniline nanofibre supported platinum (Pt) nanoelectrocatalyst is developed for direct methanol fuel cells (DMFCs). Polyaniline nanofibres (PaniNFs) with a 60 nm diameter are synthesized by a scalable interfacial polymerization without the use of a template or functional dopant. PaniNF supported Pt electrocatalyst (Pt/PaniNFs) and carbon black supported Pt electrocatalyst (Pt/C) are prepared by an ethylene glycol (EG) reduction method. The Pt nanoparticles deposited onto PaniNFs have a smaller diameter (1.8 versus 2.3 nm by XRD) and narrower particle size distribution (1.5–3 nm versus 1–5 nm by TEM) than the Pt nanoparticles deposited onto carbon black. The Pt/PaniNFs catalyst shows a higher electrochemical active surface area (ECSA) and higher methanol oxidation reaction (MOR) catalytic activity than the Pt/C.

(Some figures in this article are in colour only in the electronic version)

1. Introduction

Recently, direct methanol fuel cells (DMFCs) have been attracting enormous research interest as portable power sources because of their high energy density, fuel portability, and low operating temperature [1, 2]. However, poor methanol oxidation at the anode and methanol crossover from the anode to cathode remain to be two of the main challenges for the commercial application of DMFC [3]. The origin of the poor methanol oxidation is the sluggish electro-oxidation of adsorbed carbon monoxide, an intermediate of the anodic methanol oxidation. To improve the anode catalyst performance, there are two major strategies [3]. First, new catalyst materials must continue to be explored. Various Pt-based binary, ternary, and even quaternary compounds are being intensively investigated to increase the catalytic activity of methanol oxidation [2–5]. Second, catalytic supporting materials must be developed to achieve high dispersion, utilization, activity, and stability [3]. This approach is

particularly important for lowering the fuel cell cost by reducing the use of expensive Pt-based noble metal catalysts. A suitable supporting material must be stable in acid media, have good electric conductivity, and high specific surface area. An anisotropic morphology is also helpful in improving mass transport properties in the catalyst layer. Motivated by these considerations, we study here the use of polyaniline nanofibres (PaniNFs) as an electrocatalyst support.

Over the past several years, the majority of the electrocatalyst support research has focused on the use of carbon materials [6–16]. Recently, attention has also been given to the use of conductive polymers as electrocatalyst supports and promising results have been obtained [17–19]. By suitably combining conductive polymer and metal nanoparticles, new electrocatalysts, with higher surface areas and enhanced methanol oxidation activity, can be generated. These composite materials have demonstrated low electrical resistance in the polymer matrix during electrochemical processes [20]. In this study, we chose polyaniline because it (i) is easy to synthesize in an aqueous

---

[1] Author to whom any correspondence should be addressed.

medium, (ii) is stable over a relatively wide potential range, (iii) has a high accessible surface area, and (iv) is a good electron conductor. Many studies have explored the polyaniline supported metal nanoparticles for catalysis and sensor applications [18, 21–25]. It has been shown that nanostructured polyanilines can significantly enhance the charge transport across the electrode/electrolyte interface and thus the electronic conductivity [20, 25–29]. The first attempt of the use of polyaniline tubes (200 nm outer diameter) in fuel cells showed promise [26], however, several barriers remain to be overcome. (1) Polyaniline tubes were large in diameter and prepared by the hard template (alumina membrane) method, which increases catalyst cost and makes scale-up difficult. (2) The Pt particles deposited by the electrodeposition method have a large particle size (>20 nm), whereas a small Pt particle size (<5 nm) is desired for reducing Pt loading and improving catalytic activity. It has been found that it is always difficult to obtain small and uniform Pt particles by the electrodeposition method [3]. These considerations make it clear that a simple and scalable synthesis method for polyaniline nanofibre or nanotube, and a deposition method for producing small Pt nanoparticles (<5 nm) must be developed for the application of polyaniline as catalyst support in DMFC.

To address these concerns, the following study details a scalable synthesis method that produces thin polyaniline nanofibres (60 nm), and a novel technique for the deposition of small Pt nanoparticles (1–3 nm) on polyaniline nanofibres. Specifically the polyaniline nanofibres were prepared by interfacial polymerization without the need of a template or functional dopant [30, 31]. The Pt nanoparticles (1–3 nm) were then attached to the polyanaline nanofibres using an ethylene glycol (EG) reduction method. The methanol oxidation reaction (MOR) activity of Pt nanoparticles supported on polyaniline nanofibres (Pt/PaniNFs) was then compared with carbon black (Vulcan XC-72) supported Pt catalyst (Pt/C).

2. Experimental section

2.1. PaniNFs synthesis

All chemicals were of analytical grade and used as received from Aldrich. Polyaniline nanofibres were synthesized through an interfacial method [30]. 3.2 mmol aniline was added to 20 ml chloroform in a 100 ml glass vial. Ammonium peroxydisulfate (0.8 mmol) was dissolved in 20 ml of 1 M sulfuric acid in a 50 ml glass vial. Then the ammonium peroxydisulfate solution was poured into the aniline solution and kept at room temperature overnight. The polyaniline nanofibres were collected by filtration (Whatman Nylon Membranes, 200 nm filter) followed by washing with 500 ml double de-ionized (DDI) water.

2.2. Pt/PaniNFs preparation

As shown in figure 1, Pt/PaniNFs and Pt/C catalysts were prepared by an ethylene glycol (EG) reduction method. The preparation method is briefly described below using PaniNFs as an example. 140 mg of PaniNFs was suspended in 20 ml of ethylene glycol and stirred under sonication for 10 min. A 30 ml solution of hexachloroplatinic acid in EG (2.0 mg Pt ml^{-1} EG) was added to the solution drop-wise
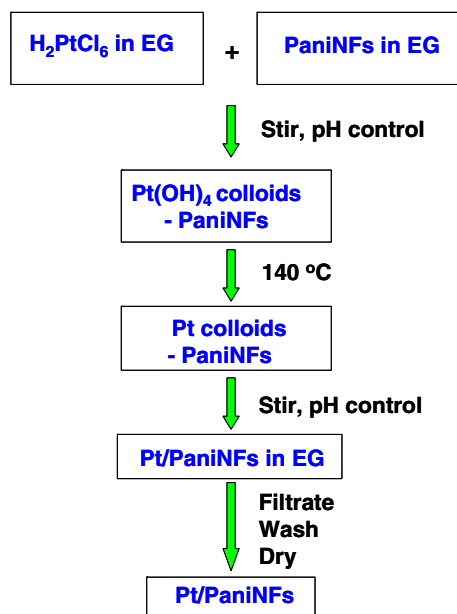

Figure 1. Schematic illustration of Pt/PaniNFs preparation procedures using the EG method.

under mechanical stirring and the stirring was continued after the Pt precursor addition for 4 h. A NaOH solution (2.5 M in EG) was added to adjust the pH of the solution to above 13, and then the solution was heated to 140 °C and kept there for 3 h. Refluxing conditions were used to keep the water in the synthesis system. The whole preparation process was conducted under flowing argon. When the solution was cooled down to room temperature, 1 M aqueous H_2SO_4 was used to adjust the pH to 2. The whole solution was then kept overnight. The product was filtered and washed with 1.5 l of DDI water (80 °C) and then dried at 70 °C for 8 h. The filtrated solvent was clear and the weight calculation showed the Pt conversion was nearly 100% during the deposition process and the Pt/PaniNFs catalysts have a metal loading of 30 wt%.

2.3. Physical characterization of Pt/PaniNFs and Pt/C

PaniNFs, Pt/PaniNFs and Pt/C powders were characterized by x-ray diffraction (XRD) on a Bruker D8 Advance Diffractometer using Cu Kα radiation with a Ni filter. The tube current was 40 mA with a tube voltage of 40 kV. The 2θ regions between $20°$ and $85°$ were explored at a scan rate of $5°$ min^{-1}. Transmission electron microscopy (TEM) was carried out on a PHILIPS CM300 operating at 200 kV. Scanning electron microscopy (SEM) was conducted on a PHILIPS XL30-FEG with an operating voltage of 7.5 kV.

2.4. Electrochemical characterization of Pt/PaniNFs and Pt/C

The methanol oxidation reaction (MOR) activity of the Pt/PaniNFs and Pt/C catalyst was conducted in a rotating disc electrode (RDE) setup using an Ag/AgCl reference electrode, and a platinum wire counter electrode. The RDE working electrode was prepared as follows. A mixture containing 8 mg of Pt/PaniNFs powder and 4 ml of ethanol was ultrasonically blended in a glass vial for half an hour. A volume of 10 μl of
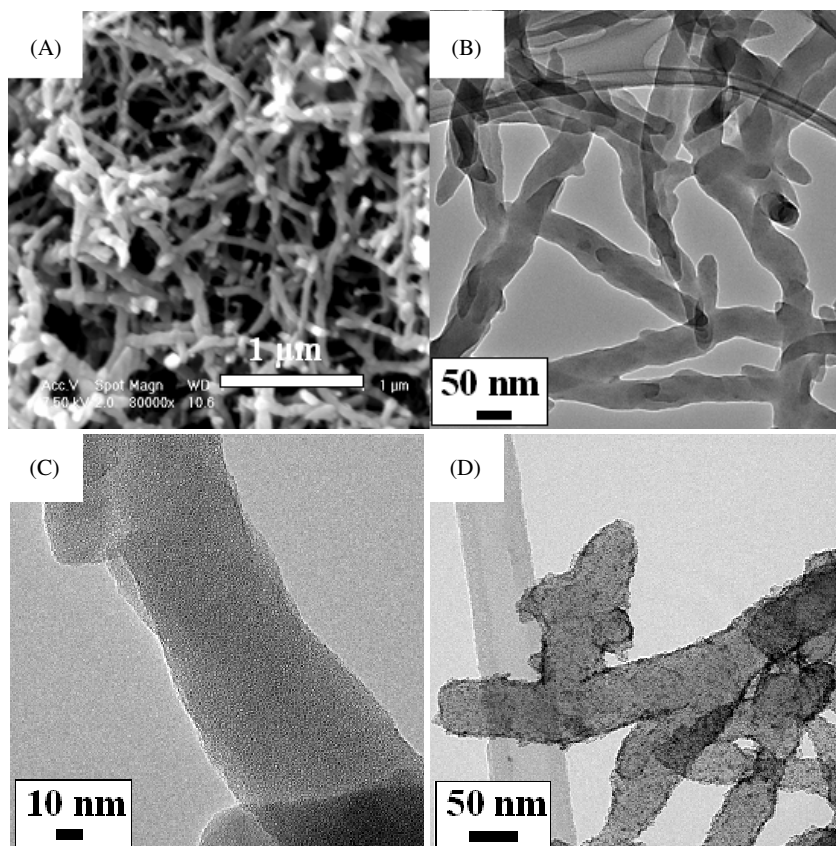
Figure 2. Scanning electron microscopy (SEM) image of PaniNFs (A) and transmission electron microscope (TEM) images of PaniNFs ((B), (C)) and Pt/PaniNFs (D).

this ink was spread on the surface of a vitreous carbon RDE ($0.196\ \text{cm}^2$) using a microsyringe and dried in a convection oven at 80 °C for about 10 min to obtain a thin active layer. After drying, about 10 μl of 0.1 wt% Nafion solution was added using the syringe. Finally, DDI water was added on the catalyst surface to check if air bubbles occur. Care was taken to make sure that no bubble formed on the surface. To confirm the reproducibility of the results, three electrodes were prepared and tested for each catalyst. The cyclic voltammetry (CV) tests were obtained in 0.5 M H_2SO_4 after nitrogen bubbling for 10 min. The scan range was from -0.15 to 1.15 V versus Ag/AgCl and the scan rate was 50 mV s^{-1}. For MOR, it was obtained in 0.5 M H_2SO_4 and 2 M CH_3OH solution after nitrogen bubbling for 10 min. The scan range was from -0.1 to 1.0 V versus Ag/AgCl and the scan rate was 50 mV s^{-1}.

3. Results and discussion

The SEM image (figure 2(A)) shows that uniform PaniNFs with a diameter about 60 nm were fabricated successfully by the interfacial polymerization method. The fibres were also examined by TEM (figures 2(B) and (C)). A typical TEM image of the Pt/PaniNFs is shown in figure 2(D). Comparing the TEM images of PaniNFs (figures 2(B) and (C)) with Pt/PaniNFs (figure 2(D)), it is clear that the Pt nanoparticles were deposited on the PaniNFs successfully. Typical TEM images of Pt/C show that Pt nanoparticles with a diameter from

1 to 5 nm were uniformly dispersed onto the carbon black (Pt/C) (figures 3(A) and (C)). In contrast, smaller and more uniform Pt nanoparticles (1.5 to 3 nm) were deposited onto the PaniNFs (figures 3(B) and (D)), which is possibly due to the unique surface properties of the PaniNFs.

The XRD patterns were collected for the Pt/PaniNFs and Pt/C samples and are shown in figure 4(A). The diffraction peak observed at $2\theta < 35°$ is attributed to the carbon and polyaniline supports. The diffraction peaks at $2\theta > 35°$ show that Pt nanoparticles are present in the face-centred cubic (fcc) structure, as indicated by the characteristic peaks of (111), (200), (220) and (311). The mean Pt particle size for the Pt/C and Pt/PaniNFs catalysts was calculated from the broadening of the (220) diffraction peaks using the Scherrer equation.

$$d = \frac{k\lambda}{B_{2\theta}\cos\theta} \tag{1}$$

where k is a coefficient (0.9), λ is the wave length of the x-ray (1.540 56 Å), $B_{2\theta}$ is the full-width half-maximum of respective diffraction peak (rad), and θ is the angle at the position of peak maximum (°).

The calculated mean Pt particle sizes for Pt/C and Pt/PaniNFs are 2.3 nm (figure 4(B)) and 1.8 nm (figure 4(C)), respectively. The XRD results are consistent with the TEM observations (figures 3(C) and (D)). Both the XRD and the TEM results suggest that by using the PaniNFs, smaller and more uniform Pt nanoparticles can be produced.
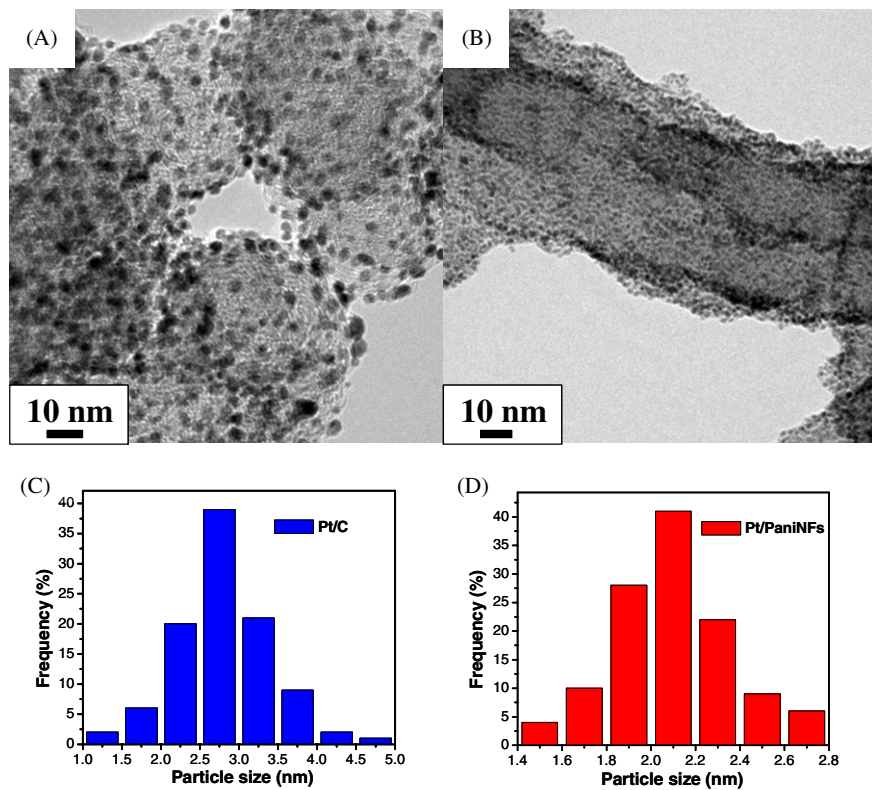
Figure 3. Transmission electron microscope (TEM) images of Pt/C (A) and Pt/PaniNFs (B); histogram of Pt nanoparticle diameter of Pt/C (C) and Pt/PaniNFs (D).
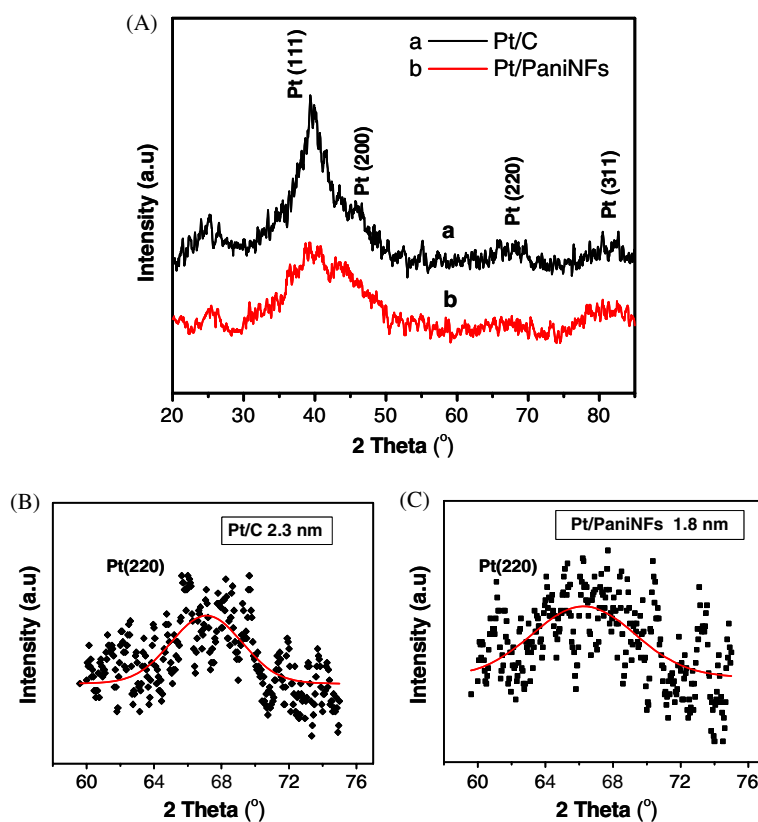

Figure 4. X-ray diffraction (XRD) patterns of Pt/C and Pt/PaniNFs (A); magnified Pt(220) diffraction peak with Gaussian fitting curve of Pt/C (B) and Pt/PaniNFs (C).
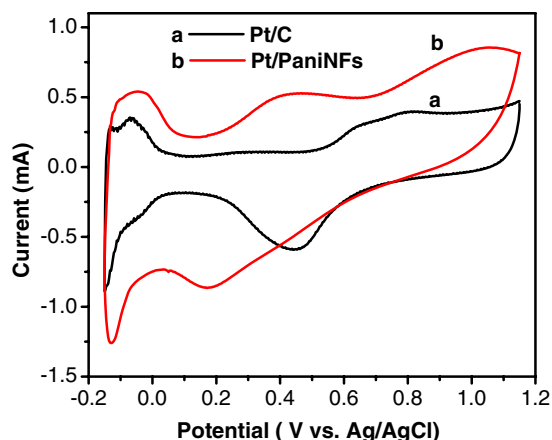
Figure 5. Cyclic voltammograms for Pt/C (a) and Pt/PaniNFs (b) in nitrogen saturated H_2SO_4 (0.5 M) by a rotating disc electrode system at a scan rate of 50 mV s^{-1}.

Figure 6. Cyclic voltammograms of Pt/C (a) and Pt/PaniNFs (b) in 1 M CH_3OH + 0.5 M H_2SO_4, at a scan rate of 50 mV s^{-1}.

Figure 5 shows the cyclic voltammetry (CV) plot of Pt/C and Pt/PaniNFs. The Pt/PaniNFs catalyst produced a higher current than Pt/C in the hydrogen region (-0.15–0.2 V versus Ag/AgCl). This result is believed to be due to the higher dispersion and smaller Pt nanoparticles of the Pt/PaniNFs catalyst. The area of adsorption or desorption of atomic hydrogen on the curve of the cyclic voltammogram has been frequently used to estimate the surface area of catalysts. The cathodic and the anodic peaks appearing between -0.15 and 0.2 V versus Ag/AgCl originated from H-adsorption and H-desorption in acidic media. By using the charge passed for H-desorption Q_H, the electrochemically active surface area (ECSA) of platinum can be estimated [32]:

$$ECSA = \frac{Q_H}{m \cdot c} \qquad (2)$$

where Q_H is the charge for hydrogen desorption (mC cm^{-2}), m is the Pt loading (mg cm^{-2}) in the electrode, and c is the charge required to oxidize a monolayer of hydrogen on Pt (0.21 mC cm^{-2}). The electrochemical active areas of platinum of Pt/PaniNFs and Pt/C electrode calculated by the above equation are 68.7 and 51.1 m^2 g^{-1}, respectively. The Pt/PaniNFs have larger ECSA than Pt/C, mainly due to the smaller and more uniform Pt nanoparticles and the possibly special morphology and properties of PaniNFs.

Methanol oxidation reaction (MOR) activity in a half cell configuration using an RDE setup (figure 6) shows the variation of performance of methanol oxidation current densities with Pt/C (curve a) and Pt/PaniNFs (curve b). The voltammetric features are in good agreement with the literature [6, 33–36], in which the typical methanol oxidation current peak on Pt catalyst is at about 0.70 V versus Ag/AgCl in the forward scan. It is evident that for the Pt/PaniNFs, the methanol oxidation starts at lower potential and the forward anodic peak current density of methanol oxidation is nearly 2 times higher than the Pt/C. In other words, the Pt/PaniNFs catalyst can generate higher currents, and thus have a higher specific activity than Pt/C catalysts. In the reverse scan, an anodic peak current density was detected at around 0.47 V, which is primarily associated with the removal of
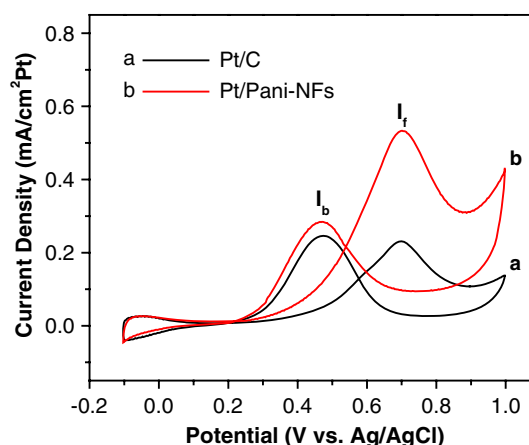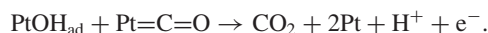
the incompletely oxidized carbonaceous species formed in the forward scan [37, 36, 38–40]. These carbonaceous species are mostly in the form of linearly bonded Pt=C=O, which are oxidized in the reaction of the backward scan peak:

$$PtOH_{ad} + Pt=C=O \rightarrow CO_2 + 2Pt + H^+ + e^-.$$

Hence, the ratio of the forward anodic peak current density (I_f) to the reverse anodic peak current density (I_b), I_f/I_b, can be used as an index of the catalyst tolerance to the carbonaceous species [35–39]. A higher I_f/I_b ratio indicates better oxidation of methanol to carbon dioxide during the anodic scan and less accumulation of carbonaceous residues on the catalyst surface. The I_f/I_b ratio of Pt/PaniNFs is 1.90, higher than that of the Pt/C catalyst (0.93), which demonstrates better tolerance of Pt/PaniNFs. The better catalytic activities and tolerance may be attributed to the unique properties and morphology of PaniNFs, which are still unclear at this time, and further investigations are needed. The half cell results suggest that Pt/PaniNFs catalysts would be a good anode catalyst candidate for DMFC.

4. Conclusions

In summary, polyaniline nanofibres with a diameter of 60 nm were prepared by a scalable chemical polymerization method. A novel Pt/PaniNFs nanoelectrocatalyst with smaller and more uniform Pt nanoparticles was successfully synthesized by the EG reduction method. The Pt/PaniNFs catalyst shows higher electrocatalytic activity and catalyst tolerance for the methanol oxidation reaction than that of the Pt/C catalyst. The Pt/PaniNFs is a promising candidate for the anode catalyst of a DMFC.

Acknowledgments

References

[1] McNicol B D, Rand D A J and Williams K R 1999 *J. Power Sources* **83** 15–31

[2] Ren X, Zelenay P, Thomas S, Davey J and Gottesfeld S 2000 *J. Power Sources* **86** 111–6

[3] Liu H, Song C, Zhang L, Zhang J, Wang H and Wilkinson D P 2006 *J. Power Sources* **155** 95–110

[4] Wasmus S and Kuver A 1999 *J. Electroanal. Chem.* **461** 14–31

[5] Liao S J, Holmes K A, Tsaprailis H and Birss V I 2006 *J. Am. Chem. Soc.* **128** 3504–5

[6] Yu J S, Kang S, Yoon S B and Chai G 2002 *J. Am. Chem. Soc.* **124** 9382–3

[7] Bessel C A, Laubernds K, Rodriguez N M and Baker R T K 2001 *J. Phys. Chem.* B **105** 1115–8

[8] Girishkumar G, Vinodgopal K and Kamat P V 2004 *J. Phys. Chem.* B **108** 19960–6

[9] Li W Z, Liang C H, Qiu J S, Zhou W J, Han H M, Wei Z B, Sun G Q and Xin Q 2002 *Carbon* **40** 791–4

[10] Li W Z, Wang X, Chen Z W, Waje M and Yan Y S 2005 *Langmuir* **21** 9386–9

[11] Park K W, Sung Y E, Han S, Yun Y and Hyeon T 2004 *J. Phys. Chem.* B **108** 939–44

[12] Wang C, Waje M, Wang X, Tang J M, Haddon R C and Yan Y S 2004 *Nano Lett.* **4** 345–8

[13] Wang X, Waje M and Yan Y S 2005 *Electrochem. Solid-State Lett.* **8** A42–4

[14] Su F B, Zeng J H, Bao X Y, Yu Y S, Lee J Y and Zhao X S 2005 *Chem. Mater.* **17** 3960–7

[15] Li W Z, Liang C H, Zhou W J, Qiu J S, Zhou Z H, Sun G Q and Xin Q 2003 *J. Phys. Chem.* B **107** 6292–9

[16] Waje M M, Wang X, Li W Z and Yan Y S 2005 *Nanotechnology* **16** S395–400

[17] Kost K M, Bartak D E, Kazee B and Kuwana T 1988 *Anal. Chem.* **60** 2379–84

[18] Kessler T and Luna A M C 2003 *J. Solid State Electrochem.* **7** 593–8

[19] Hable C T and Wrighton M S 1993 *Langmuir* **9** 3284–90

[20] Vandyke L S and Martin C R 1990 *Langmuir* **6** 1118–23

[21] Li W S, Lu J, Du J H, Lu D S, Chen H Y, Li H and Wu Y M 2005 *Electrochem. Commun.* **7** 406–10

[22] Kitani A, Akashi T, Sugimoto K and Ito S 2001 *Synth. Met.* **121** 1301–2

[23] Niu L, Li Q H, Wei F H, Wu S X, Liu P P and Cao X L 2005 *J. Electroanal. Chem.* **578** 331–7

[24] Planes G A, Rodriguez J L, Pastor E and Barbero C 2003 *Langmuir* **19** 8137–40

[25] Rajesh B, Thampi K R, Bonard J M, Xanthapolous N, Mathieu H J and Viswanathan B 2002 *Electrochem. Solid-State Lett.* **5** E71–4

[26] Rajesh B, Thampi K R, Bonard J M, Mathieu H J, Xanthopoulos N and Viswanathan B 2004 *Electrochem. Solid-State Lett.* **7** A404–7

[27] Bensebaa F, Farah A A, Wang D S, Bock C, Du X M, Kung J and Le Page Y 2005 *J. Phys. Chem.* B **109** 15339–44

[28] Zhang L J and Wan M X 2002 *Nanotechnology* **13** 750–5

[29] Kim B K, Kim Y H, Won K, Chang H J, Chi Y M, Kong K J, Rhyu B W, Kim J J and Lee J O 2005 *Nanotechnology* **16** 1177–81

[30] Huang J X and Kaner R B 2004 *J. Am. Chem. Soc.* **126** 851–5

[31] Huang J X and Kaner R B 2004 *Angew. Chem. Int. Edn* **43** 5817–21

[32] Pozio A, De Francesco M, Cemmi A, Cardellini F and Giorgi L 2002 *J. Power Sources* **105** 13–9

[33] Liang H P, Zhang H M, Hu J S, Guo Y G, Wan L J and Bai C L 2004 *Angew. Chem. Int. Edn* **43** 1540–3

[34] Guo D J and Li H L 2004 *J. Electroanal. Chem.* **573** 197–202

[35] Mu Y Y, Liang H P, Hu J S, Jiang L and Wan L J 2005 *J. Phys. Chem.* B **109** 22212–6

[36] Liu Z L, Ling X Y, Su X D and Lee J Y 2004 *J. Phys. Chem.* B **108** 8234–40

[37] Manoharan R and Goodenough J B 1992 *J. Mater. Chem.* **2** 875–87

[38] Yajima T, Uchida H and Watanabe M 2004 *J. Phys. Chem.* B **108** 2654–9

[39] Zhu Y M, Uchida H, Yajima T and Watanabe M 2001 *Langmuir* **17** 146–54

[40] Huang J C, Liu Z L, He C B and Gan L M 2005 *J. Phys. Chem.* B **109** 16644–9